

# Origin of periodic and chaotic dynamics due to drops moving in a microfluidic loop device

Jeevan Maddala, Siva A. Vanapalli, and Raghunathan Rengaswamy

Department of Chemical Engineering, Texas Tech University, Lubbock, Texas 79401-3121, USA

(Received 7 February 2013; published 26 February 2014)

Droplets moving in a microfluidic loop device exhibit both periodic and chaotic behaviors based on the inlet droplet spacing. We observe that the periodic behavior is an outcome of carrier phase mass conservation principle, which translates into a *droplet spacing quantization rule*. This rule implies that the summation of exit spacing is equal to an integral multiple of inlet spacing. This principle also enables identification of periodicity in experimental systems with input scatter. We find that the origin of chaotic behavior is through intermittency, which arises when drops enter and leave the junctions at the same time. We derive an analytical expression to estimate the occurrence of these chaotic regions as a function of system parameters. We provide experimental, simulation, and analytical results to validate the origin of periodic and chaotic behavior.

DOI: [10.1103/PhysRevE.89.023015](https://doi.org/10.1103/PhysRevE.89.023015)

PACS number(s): 47.55.D-, 47.20.Ky, 47.10.ab, 47.27.ed

Motion of droplets in a microfluidic loop device is a very simple phenomenon that exhibits complex spatiotemporal dynamics [1,2]; such phenomena are rare in practice [3]. It has been shown that a train of droplets entering the loop at fixed inlet spacing could exit the loop at periodic or chaotic time intervals [1,4–6]. While the rules governing the droplets' motion are uncomplicated, discrete decision-making at bifurcations and collective hydrodynamics lead to intricate dynamics [2]. This contrast between the simplicity of the device and the plurality of its response has resulted in this system being investigated by several researchers [5–9]. Despite these investigations the dynamics of drop traffic in a loop is not fully understood. In this paper, we address the following three questions: (i) What are the origins of the periodic and chaotic behavior? (ii) How does the system transition between these behaviors? (iii) Is it possible to predict the regions of periodic and chaotic behavior? Addressing these questions is not only important for the design of drop-based fluidic devices [1,2,5,10] but more broadly has relevance in understanding how decision-making leads to multistability and memory storage [7,11] in biological networks [12,13].

Consider a train of droplets entering a microfluidic loop device as shown in Fig. 1 at a constant inlet spacing  $\lambda$ . The relative spacings between the droplets remain constant until they reach the loop junction. As the droplets enter the upper or lower branch, the hydraulic resistance of that branch changes. This results in a redistribution of the bulk flows to the upper and lower branches. Since the droplets' velocities are proportional to the bulk flow rate, the droplets in the upper and lower branches move at different velocities leading to changes in the relative distances between them as they exit the loop.

The loop device ( $G$ ) transforms the spacings of a sequence of  $n$  droplets at the inlet ( $\{\lambda\}_n$ ) to an exit sequence,  $\{\bar{\lambda}\}_n = \{G(\lambda)\}_n$ . It has been shown in the literature that the exit spacings can either form a periodic or a chaotic pattern [5,6]. These patterns are captured through a Poincaré map, where the number of distinct clusters represent the number of periods. There are two disadvantages to such a characterization: it is difficult to exactly identify the number of periods when confronted with scatter in the data due to noise in the experiments, and the Poincaré map does not explain the physics of the process that leads to these periodic or aperiodic behaviors. To address these two issues, we start with a mathematical

definition of periodicity. The exit sequence ( $\{\bar{\lambda}\}_n$ ) is periodic with period  $p$ , where  $p$  is the smallest positive integer such that  $\{\bar{\lambda}\}_i = \{\bar{\lambda}\}_{i+p} \forall i \in \mathbb{N}$ . The exit sequence is aperiodic, if there exists no  $p$  such that  $\{\bar{\lambda}\}_i = \{\bar{\lambda}\}_{i+p} \forall i \in \mathbb{N}$ . From the definition of periodicity it can be noticed that the periodicity condition will hold for all integer multiples of  $p$ . Further, it is self-evident that the periodicity condition cannot hold for two  $p$ 's that are not multiples of each other. However, if the periodicity condition is valid in some region, i.e.,  $i \in (N_1, N_2)$  for some  $p$ , then that behavior is termed locally periodic. We are interested in the physics that leads to periodic behavior and the manner in which the system transitions from periodic to chaotic behavior and vice versa.

The sustained periodic behavior is a result of a series of droplets taking the same decisions repeatedly—this can also be viewed as memory of the system [7]. The decisions will be repeated with period  $p$  if the  $i$ th and  $(i + p)$ th droplets undergo the same experience, i.e., velocity-changes as they pass through the loop. This happens if the loop snapshot (i.e., instantaneous droplet configurational positions in the loop) encountered by the  $(i + p)$ th and the  $i$ th drop are same, which results in an average relative velocity between these drops to be zero. A natural consequence of this concept is that the amount of the carrier phase fluid trapped between the  $i$ th and  $(i + p)$ th droplets at the exit should exactly equal the amount of the fluid trapped between the same droplets prior to entering the loop. Mathematically, the carrier fluid present in between  $i$ th and  $(i + p)$ th droplets prior to the device entry is  $p\lambda S$ , where  $S$  is the cross-sectional area of the channel. Assuming bulk phase incompressibility, the volume trapped between the droplets after exit is the sum of all the exit relative spacings multiplied by  $S$ . This volume conservation that is required for repetition translates to a remarkable “quantization of droplet spacing (QDS)” given below:

$$\bar{\lambda}_{i+1} + \bar{\lambda}_{i+2} + \cdots + \bar{\lambda}_{i+p} = p\lambda. \quad (1)$$

If there exists a unique  $p$ ,  $\forall i \in \mathbb{N}$  then Eq. (1) is an “if and only if” condition for a loop device to show sustained periodic oscillations. We validate this QDS principle that is derived through physical arguments using network model [1]. Confined droplet dynamics is predicted using the network model under the assumption that the droplets do not collide

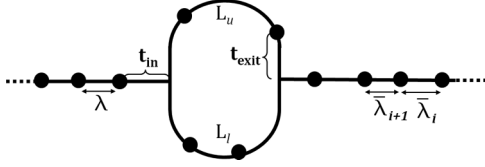


FIG. 1. A stream of droplets with constant inlet spacing passing through a microfluidic loop device; We used  $L_u = 2235 \mu\text{m}$  and  $L_l = 2217 \mu\text{m}$  in our simulations and experiments.

[14]. The network model has been shown to satisfactorily predict the droplet dynamics in microfluidic loop [15] and ladder networks [16,17]. In this model, drops are treated as point objects moving at a velocity  $v = \beta Q/S$  [18–20], where  $\beta$  is the slip factor,  $S$  is the cross-sectional area, and  $Q$  is the flow rate.  $L_l$  and  $L_u$  are the length of upper and lower branches, respectively, as shown in Fig. 1. Droplets decisions at the bifurcation depend on the maximum instantaneous flow rate. If same number of drops exist in both the branches, the entering droplet always chooses the lower branch because it is assumed to be slightly shorter than the upper branch. This slight asymmetry ensures that the droplet decisions are deterministic. The resistance of the branch is summation of the resistance of the channel [15] and resistance due to drops ( $nR_d$ ), where  $n$  is the number of drops in the branch and  $R_d$  is the excess hydrodynamical resistance per drop. Using this network model, we illustrate the QDS principle with two representative scenarios: 3-period and 9-period behaviors, without input fluctuations. Motivated by Eq. (1), we plot the

value of  $|\Sigma_{i+1}^{i+j} \bar{\lambda} - j\lambda|/\lambda$  as a function of  $j$  as shown in Fig. 2. If the QDS rule is correct then this value should be equal to zero whenever  $j$  is equal to multiples of  $p$ , the periodicity of the system. The initial  $i$  that is used in the equation does not have any impact on the result because the case studies considered here have sustained periodic oscillations. As expected, in Fig. 2, the curve touches the  $x$  axis at  $N = 3, 6, 9 \dots$  for the 3-period case and  $N = 9, 18 \dots$  for the 9-period case, validating the carrier phase conservation principle.

We now validate QDS principle using an experimental system; but estimation of the period  $p$  in case of experiments can be complicated due to fluctuations in the inlet spacing. In such cases using Poincaré maps [2] to obtain periodicity may be misleading. The conservation principle provides another view of periodicity. Looking at Eq. (1), it is apparent that the periodicity is equal to the number of droplets that exit before a snapshot repeats because these many droplets participate in the conservation equation. Consider a seemingly 2-period behavior as identified by a Poincaré map in Fig. 2(b), which was obtained experimentally. Modeling the system without experimental fluctuations at the inlet using experimentally measured  $R_d$  and  $\beta$  values leads to a 3-period behavior. To confirm if this is the true period of the system we used the snapshot comparison technique derived from the QDS principle. The 1st image is repeated after the 132nd and 264th snapshots as shown in Fig. 2(c). In this case, three droplets exit between 1st, 132nd, and 264th images, confirming that this indeed is 3-period behavior, contrary to what Poincaré map suggests. Thus, the QDS principle is extremely useful in determining the true periodicity of loop dynamics where

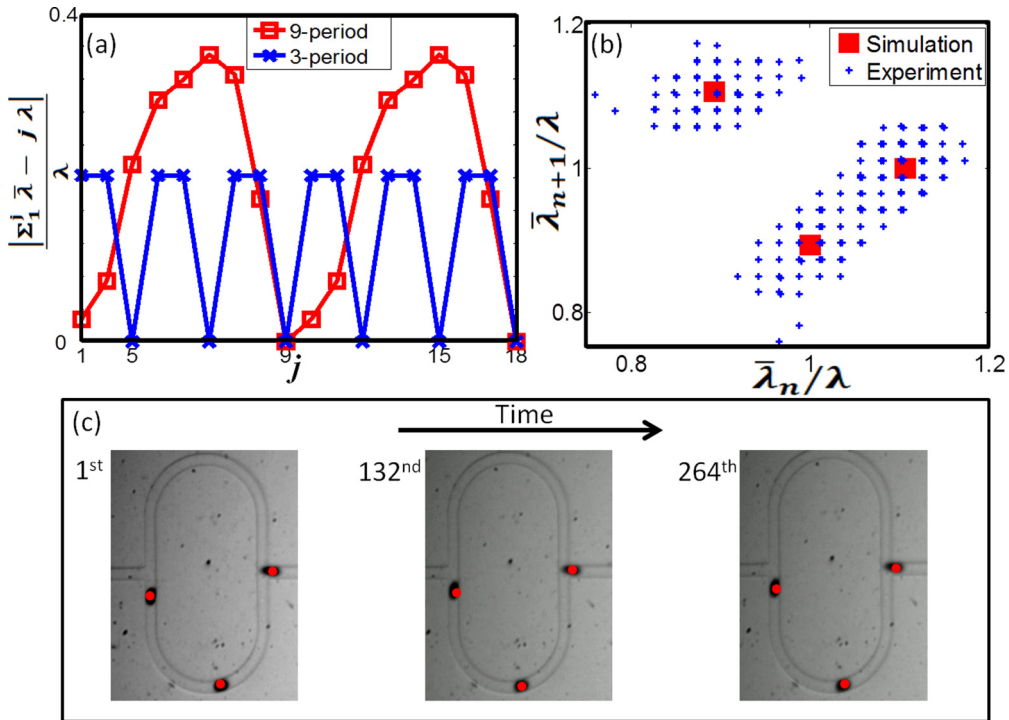


FIG. 2. (Color online) Periodic behavior: (a) Quantization of droplet spacing in the cases of 3- and 9-period behaviors. (b) Poincaré map shows a 2-period behavior, whereas simulation and experiment show a 3-period behavior, at oil and water flow rates of  $Q_o = 550$  and  $Q_w = 25 \mu\text{L/hr}$ ;  $R_d/R_l = 0.1$  and  $\beta = 1.4$  is used in the simulation. (c) It is observed that in experimental snapshots (1st, 132nd, and 264th), three droplets exit the loop device before the images repeat.

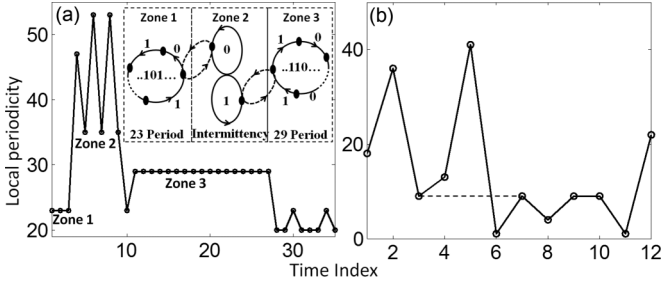


FIG. 3. Periodicity ( $p$ ) calculated using Eq. (1) for an aperiodic system at distinct intervals of time index ( $I$ ) shows: (a) a simulated system showing intermittency between zone 1 and zone 3 for a particular inlet spacing  $\lambda/L_i = 0.99$ ;  $R_d/R_l = 0.15$ ; the inset shows a graph diagram depicting these transitions due to binary decisions in the loop device; (b) an aperiodic experimental system demonstrating similar behavior;  $Q_o = 250$  and  $Q_w = 25 \mu\text{L/h}$ .

experimental scatter might otherwise make such identification problematic.

We now turn our attention to the understanding of aperiodic behavior and the physics that leads to the transitions from periodic to aperiodic behavior and vice versa. A deterministic system resulting in aperiodic behavior with sensitivity to initial conditions is defined as chaos [21]. If the loop system  $G$  shows these characteristics then the loop system is said to be chaotic. We use a Lyapunov exponent to observe the sensitivity to initial conditions. In the works presented in the literature, experiments and simulations have been conducted varying the inlet spacing to predict these transition regions. In our work, to understand the origins for these transitions we performed simulations and experiments at a *fixed* inlet spacing where the dynamics was chaotic and followed the time evolution of the exit spacing. The simulations are performed with a deterministic network model without any experimental uncertainties. To identify the origin of these transitions, we explore what happens to the conservation principle in the aperiodic region.

In Fig. 3(a), the  $x$  axis of the plot is increasing natural numbers ( $I$ ) representing the  $I$ th time that the QDS principle was obeyed in the outlet sequence of the simulation. The  $y$  axis denotes the number of droplets that participate in the QDS equation (which is the measure of periodicity  $p$ ) when it holds for the  $I$ th time. This plot suggests that even in the aperiodic case, the conservation principle is still driving the physics; however, the periodicity changes with time and the conservation equation is valid at all these periodicities. Zone 1 in Fig. 3 shows an initial period of 23, where for a while a local periodic behavior is observed, which is broken by a burst of intermittent behavior as observed in Zone 2 then transitioning to a 29-period; this is a classic case of intermittency [21]. Notice, however, the subtle distinction between globally periodic and locally periodic behaviors. In the former case, snapshots have to repeat, whereas in the latter case, the snapshots need not repeat. The intermittent appearance of periodic behavior in an aperiodic scenario is depicted graphically in the inset of Fig. 3(a), where the values “0” and “1” represent the binary decisions of the droplets, i.e., choice of either the upper or the lower branch. In the transition

regions any combination of 0’s and 1’s is possible. This can result in large intermittent periods and sporadic transitions to other periodic behaviors similar to the phenomena observed in Zone 2 of the simulation. Note that the simulations are performed with no uncertainty.

We now ask if this intermittent behavior leads to chaos? We define a Lyapunov exponent similar to Behzad *et al.* [6], as follows:

$$L = \frac{1}{s} \log \left[ \frac{\Delta \lambda_s}{\Delta \lambda} \right]. \quad (2)$$

The Lyapunov exponent  $L$  is calculated after a very long train of  $s$  droplets exit the loop device. The inlet spacing ( $\lambda$ ) is perturbed by a factor of  $10^{-5}$  times ( $\lambda$ ) and  $\Delta \lambda = \lambda_{\text{original}} - \lambda_{\text{perturbed}}$ . In the transition regions the Lyapunov exponent is positive and in the periodic regime  $L \approx 0$ . A positive Lyapunov exponent implies that the loop system is sensitive to initial conditions, whereas a zero Lyapunov exponent implies the system has a stable cycle and is conservative. The microfluidic loop simulation starts with zero drops in the loop device, hence there will be initial transitions in the exit spacing. These transitions attenuate down and the system settles to a stable cycle in the case of periodic dynamics, while in an aperiodic region, the system transitions from one cycle to another. Therefore, the loop system never settles down to a stable cycle in the transition regions; this is observed in Fig. 3(a). The system shows local periodic behavior, but the snapshots do not repeat exactly as in the globally periodic regions. The positive Lyapunov exponent along with aperiodic behavior observed in Fig. 3(a) shows that the loop dynamics is indeed chaotic in the transition regions.

We now understand the transitions in the loop device through experiments. Figure 3(b) shows results from an experimental system displaying aperiodic behavior where the conservation principle is valid for distinct sets of droplets. In the case of experimental systems, the inevitable noise makes it impossible to identify chaotic phenomena exactly. Since, unlike simulations, it is not possible to exactly fix the inlet spacing in experiments, it is impossible to experimentally demonstrate that even at fixed inlet spacings intermittency is exhibited. However, the natural variations in  $\lambda$  (which can be thought of as being equivalent to perturbations in the simulations) result in chaotic behavior in the experimental system in the regions predicted by the theory, whereas similar fluctuations in the periodic region does not have a significant effect and the system remains periodic. Further, the transition phenomenon mirrors the simulation results as seen in Fig. 3(b). Therefore, through simulations and experiments, we understand that transitions lead to chaos through an intermittency route. Our analysis further suggests that the aperiodic behavior is likely to be interspersed between the periodic regimes.

We now ask how is the chaotic behavior triggered? Figure 4 shows the snapshots of experimental scenario where the chaotic behavior is observed [cf. Fig. 3(b)]. Inspection of these snapshots reveal an important insight regarding what triggers the intermittent behavior. As the exiting drop leaves, the entering drop can either take the lower or the upper branch. In the case of Fig. 4(a), the entering droplet chooses the upper branch, but in the case of Fig. 4(b), the droplet chooses the lower branch. Although the system has very

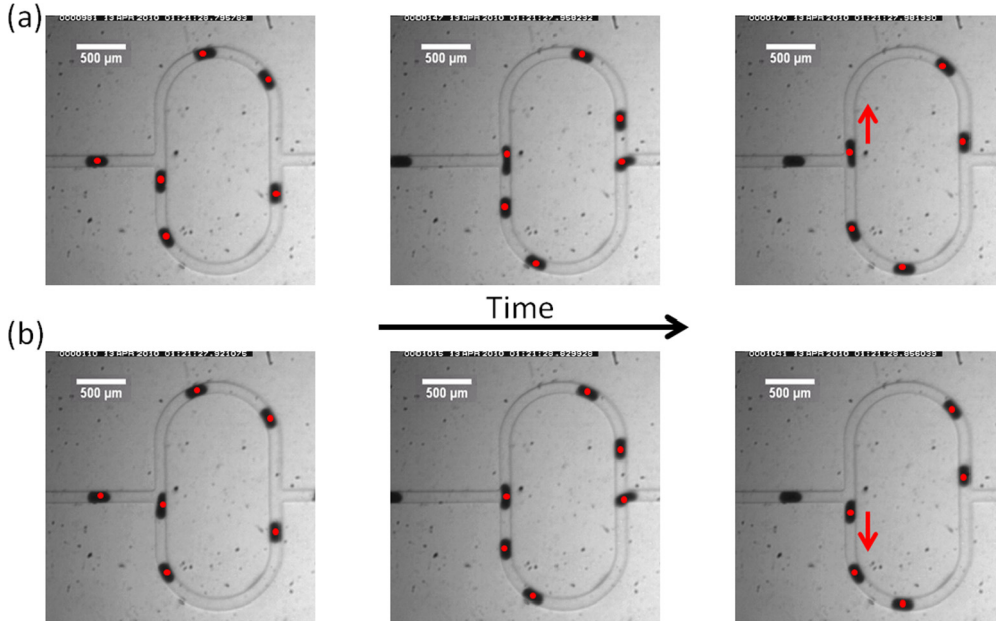


FIG. 4. (Color online) A loop device showing transitions: (a) a sequence of snapshots showing the entering droplet choosing the upper branch; (b) at a later time in the same experiment, with similar conditions, the entering droplet chooses the lower branch.  $Q_o = 250$  and  $Q_w = 25 \mu\text{L/h}$ .

similar conditions at both times, the dynamics of this system moves to a completely different regime due to a single droplet altering its decision leading to chaotic behavior. Since such transitions may happen at different time instants, the dynamics of the system becomes chaotic. For aperiodic behavior to be manifested, there has to be a critical event to break the constant periodic cycle. We conclude that this critical event is one where the droplets enter and exit at around the same time, leading to changes in the droplets' decisions. This will in turn change the amount of dispersed phase fluid trapped between the droplets.

We now focus on predicting these intermittent transitions using the important insight that simultaneous entry and exit of drops at a junction leads to chaotic behavior. To predict transition regions we simulated the dynamics for a wide range of inlet spacings using the network model. Based on input frequency, after the initial transients, the droplet exit pattern reaches a steady state. Figure 5(a) shows a bifurcation map,

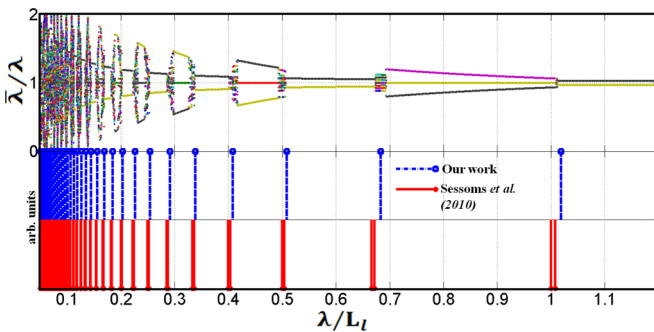


FIG. 5. (Color online) Bifurcation map simulated by changing the input spacing in a scenario where  $Q_o = 550$  and  $Q_w = 25 \mu\text{L/h}$ ,  $R_d/R_l = 0.1$ ; the bottom plot shows the prediction of transitions in the bifurcation maps using the proposed analytical expression along with that reported in the literature [5].

where normalized inlet spacing is plotted on the  $x$  axis and the normalized outlet spacing is plotted on the  $y$  axis. It is clear that there is a band of (infinite set)  $\lambda$  values in a very small range that characterizes the transition region as shown in Fig. 5(a). The width of transition band is dependent on the droplet size. In the network model, we assume droplets as point objects. The finite sizes of the droplets affect the width of the chaotic regions. As the possibility of droplets entering and exiting the loop device at the same time increases for longer droplets, we believe that the width of these transition bands will increase as the droplet size increases. Predicting the range for  $\lambda$  values in the transition band is a difficult task. We therefore attempt to predict a particular value of  $\lambda$  ( $\lambda_c$ ) in the transition region, which is still practically useful as the transition band is narrow. To predict this critical inlet spacing  $\lambda_c$ , we need to find a  $\lambda$  that results in a scenario where a droplet enters the loop while another droplet is exiting. As this could happen for several different pairs of droplets (leading to a range of  $\lambda$  values), to obtain an analytical expression, we assume that the critical  $\lambda_c$  is when the *first* droplet exits the loop while another droplet arrives at the junction. We also assume that the loop is symmetric ( $L_l \approx L_u$ ), making droplets alternate between top and bottom branches. Depending on the  $\lambda_c$ , the number of droplets that a loop holds ( $n$ ) before the first droplet exits could be different. The exit time of the first droplet after  $n$  droplets enter the loop device (shown in Fig. 1) is as follows:

$$t_{1,\text{exit}} = \frac{L_l - \sum_{k=1}^n \lambda \left\{ \frac{R_u + \text{floor}[(k-1)/2]R_d}{R_u + R_l + (k-1)R_d} \right\}}{\beta Q / S \left( \frac{R_u + R_d}{R_u + R_l + nR_d} \right)} \quad (3)$$

In Eq. (3),  $R_l$  and  $R_u$  are the branch resistances. The entry time of the  $(n+1)$ th drop in the loop is given by  $t_{\text{entry}} = \frac{\lambda S}{\beta Q}$ . Since the critical ( $\lambda_c$ ) values occur when  $t_{1,\text{exit}} = t_{\text{entry}}$ ,



we get

$$\frac{L_l}{\lambda_c} = \sum_{k=1}^n \frac{R_u}{R_u + R_l + kR_d} + \sum_{k=1}^n \frac{\text{floor}(k/2)R_d}{R_u + R_l + kR_d}. \quad (4)$$

The critical  $\lambda_c$  values are obtained by varying  $n, n \in \mathbb{N}$ . We note that the  $n$  used in the calculation of a particular transition  $\lambda_c$  does not provide any indication of the period  $p$  of the sustained periodic behavior that follows the transition. This is because the transition  $\lambda_c$  has no bearing on the number of droplets for which the conservation principle holds.

We validate Eq. (4) using a simulated bifurcation map and a recent result from literature [5]. Simulations results are shown in Fig. 5(a); at  $\lambda > 1$ , the system shows a steady 2-period behavior, but as the spacing decreases, the outlet periodicity transitions from a 2-period to a 3-period behavior—observe that there is no period doubling vis a vis logistic map [21]. This is because the transitions happen through intermittency route. The 3-period behavior lasts for some time and the system goes back to a 2-period behavior. After the next transition, the system drifts to a 4-period behavior. We observe only three values repeating within the 4-period pattern. The analytical

expression captures all these transition regions, corroborating the observation that droplets entering and exiting at the same time leads to chaotic behavior.

In conclusion, we propose a rule for quantization of droplet spacing that is valid for periodic and chaotic behavior in microfluidic loop systems. As the conservation of spacing is valid for both periodic and chaotic regions of the loop device, this device resembles a Hamiltonian system [8]. The chaotic behavior is a result of transitions occurring when droplets enter and exit at the same time. This is akin to complex sequences derived with simple rules in Ref. [22]. We derive an analytical expression for predicting the transition regions based on the new physical insights proposed in this paper. The results suggest that the system achieves chaotic behavior through a phenomenon called “intermittency route to chaos” [21,23] and not just because of a 3 -period behavior [24].

We thank Prof. Jerzy Blawdziewicz, Dr. Zeina S. Khan, and William S. Wang for valuable discussions. We also thank Dr. Babji Srinivasan and Swastika S. Bithi for experimental movies used for analysis in this paper. We acknowledge financial support from National Science Foundation (Grant No. CDI-1124814).

- 
- [1] M. Schindler and A. Ajdari, *Phys. Rev. Lett.* **100**, 044501 (2008).
  - [2] M. J. Fuerstman, P. Garstecki, and G. M. Whitesides, *Science* **315**, 828 (2007).
  - [3] P. Garstecki, M. J. Fuerstman, and G. M. Whitesides, *Nature Physics* **1**, 1745 (2005).
  - [4] B. J. Smith and D. P. Gaver III, *Lab Chip* **10**, 303 (2010).
  - [5] D. A. Sessoms, A. Amon, L. Courbin, and P. Panizza, *Phys. Rev. Lett.* **105**, 154501 (2010).
  - [6] M. D. Behzad, H. Seyed-allaei, and M. R. Ejtehadi, *Phys. Rev. Ed.* **82**, 037303 (2010).
  - [7] O. Cybulski and P. Garstecki, *Lab Chip* **10**, 484 (2009).
  - [8] R. Jeanneret, J.-P. Vest, and D. Bartolo, *Phys. Rev. Lett.* **108**, 034501 (2012).
  - [9] T. Glawdel, C. Elbuken, and C. Ren, *Lab Chip* **11**, 3774 (2011).
  - [10] M. Prakash and N. Gershenfeld, *Science* **315**, 832 (2007).
  - [11] J. Foss, A. Longtin, B. Mensour, and J. Milton, *Phys. Rev. Lett.* **76**, 708 (1996).
  - [12] D. Angeli, J. E. Ferrell, and E. D. Sontag, *Proc. Nat. Acad. Sci. USA* **101**, 1822 (2004).
  - [13] M. Leite and Y. Wang, *Math. Biosci. Eng* **7**, 83 (2010).
  - [14] M. Belloul, W. Engl, A. Colin, P. Panizza, and A. Ajdari, *Phys. Rev. Lett.* **102**, 194502 (2009).
  - [15] J. Maddala, B. Srinivasan, S. S. Bithi, S. A. Vanapalli, and R. Rengaswamy, *AIChE Journal* **58**, 2120 (2012).
  - [16] J. Maddala, W. Wang, S. Vanapalli, and R. Rengaswamy, *Microfluidics and Nanofluidics* **14**, 337 (2013).
  - [17] J. Maddala and R. Rengaswamy, *Comput. & Chem. Eng.* **60**, 413 (2014).
  - [18] S. Jakiela, P. M. Korczyk, S. Makulska, O. Cybulski, and P. Garstecki, *Phys. Rev. Lett.* **108**, 134501 (2012).
  - [19] V. Labrot, M. Schindler, P. Guillot, A. Colin, and M. Joanicot, *Biomicrofluidics* **3**, 012804 (2009).
  - [20] D. A. Sessoms, M. Belloul, W. Engl, M. Roche, L. Courbin, and P. Panizza, *Phys. Rev. E* **80**, 016317 (2009).
  - [21] S. Strogatz, *Nonlinear Dynamics and Chaos: with Applications to Physics, Biology, Chemistry, and Engineering* (Westview Press, Massachusetts, USA, 2001).
  - [22] S. Wolfram, *Nature* **311**, 419 (1984).
  - [23] E. Ott, *Chaos in Dynamical Systems* (Cambridge University Press, New York, USA, 1993).
  - [24] T.-Y. Li and J. A. Yorke, *The American Mathematical Monthly* **82**, 985 (1975).